# The receptor-like kinase SERK3/BAK1 is a central regulator of innate immunity in plants

Antje Heese*†, Dagmar R. Hann‡, Selena Gimenez-Ibanez‡, Alexandra M. E. Jones‡, Kai He§, Jia Li§, Julian I. Schroeder¶, Scott C. Peck‡‖, and John P. Rathjen†‡

*Department of Biochemistry, University of Missouri, 540G Bond Life Sciences Center,1201 Rollins Road, Columbia, MO 65211; ‡The Sainsbury Laboratory, Norwich Research Park, Colney Norwich NR4 7UH, United Kingdom; §Department of Botany and Microbiology, University of Oklahoma, Norman, OK 73019; and ¶Division of Biological Sciences, Cell and Developmental Biology, University of California at San Diego, 9500 Gilman Drive, La Jolla, CA 92093-0346

Communicated by David Baulcombe, The Sainsbury Laboratory, Norwich, United Kingdom, June 6, 2007 (received for review May 25, 2007)

**In pathogen-associated molecular pattern (PAMP)-triggered immunity (PTI), plant cell surface receptors sense potential microbial pathogens by recognizing elicitors called PAMPs. Although diverse PAMPs trigger PTI through distinct receptors, the resulting intracellular responses overlap extensively. Despite this, a common component(s) linking signal perception with transduction remains unknown. In this study, we identify SOMATIC EMBRYOGENESIS RECEPTOR KINASE (SERK)3/brassinosteroid-associated kinase (BAK)1, a receptor-like kinase previously implicated in hormone signaling, as a component of plant PTI. In *Arabidopsis thaliana*, AtSERK3/BAK1 rapidly enters an elicitor-dependent complex with FLAGELLIN SENSING 2 (FLS2), the receptor for the bacterial PAMP flagellin and its peptide derivative flg22. In the absence of *AtSERK3/BAK1*, early flg22-dependent responses are greatly reduced in both *A. thaliana* and *Nicotiana benthamiana*. Furthermore, *N. benthamiana Serk3/Bak1* is required for full responses to unrelated PAMPs and, importantly, for restriction of bacterial and oomycete infections. Thus, *SERK3/BAK1* appears to integrate diverse perception events into downstream PAMP responses, leading to immunity against a range of invading microbes.**

flg22 | *Arabidopsis* | nicotiana | Flagellin | brassinosteroid

*Arabidopsis thaliana* contains >600 receptor-like kinases (RLKs), which are transmembrane proteins with divergent extracellular domains providing ligand specificity and cytoplasmic kinase domains implicated in downstream signaling (1, 2). Although roles for most RLKs are unknown, many are implicated in plant growth and development, whereas others function in plant defense as so-called pattern-recognition receptors (PRRs) (3, 4). PRRs detect potential microbial pathogens by recognizing diverse pathogen-associated molecular patterns (PAMPs), including bacterial flagellin and cold-shock protein, fungal chitin, and oomycete INF1 (5–8). PAMP perception initiates PAMP-triggered immunity (PTI), the first line of defense contributing to arrest of microbial growth (9). Different PAMP perception events activate similar sets of responses, including a burst of active oxygen species (AOS), induction and repression of similar genes, and activation of a MAPK cascade (10, 11). Because of this convergence, the presence of a common adaptor or regulatory protein linking PAMP perception with early signaling events has been proposed, possibly by complex formation with different PRRs (4).

In *A. thaliana*, the best-studied PTI system involves recognition of the bacterial PAMP flagellin or its peptide derivative flg22 by the RLK AtFLS2 (FLS2, FLAGELLIN SENSING 2; ref. 12). Based on extensive binding and chemical cross-linking studies, this leucine-rich repeat RLK functions as a PRR that determines specificity for flg22 (13, 14). Perception of flagellin or flg22 is not species-specific, because it induces defense-related responses in distant relatives such as *Nicotiana* spp.(15, 16). In agreement, we recently identified a *Nicotiana benthamiana* gene, *NbFls2*, which is closely related to *AtFLS2* and required for flagellin perception in this species (16). Although flagellin recognition contributes specifically but weakly to PTI against bacterial growth in *A. thaliana*, growth of several bacterial strains is strongly restricted by *NbFls2* perception on *N. benthamiana* (16, 17).

Although many flg22-induced responses were characterized in detail (11, 18, 19), very little is known about components linking flg22 perception with early signaling events. Here we identified SOMATIC EMBRYOGENESIS RECEPTOR KINASE (SERK)3/brassinosteroid (BR)-associated kinase (BAK)1, a member of the SERK family (20, 21), as a factor required for early PAMP responses and importantly, PTI. Because AtSERK3/BAK1 formed a rapid flg22-elicited complex with AtFLS2, AtSERK3/BAK1 may function in linking PAMP signal perception with transduction. These results implicate SERK3/BAK1, a leucine-rich repeat RLK previously shown to function in BR signaling (22, 23) via interaction with the BR receptor BR-INSENSITIVE 1 (BRI1) (24), in both plant PTI and hormone signaling.

## Results and Discussion

**AtSERK3/BAK1 Is Required for flg22-Dependent Responses and Forms a flg22-Induced Complex with AtFLS2 in *A. thaliana*.** To identify proteins that form a flg22-elicited complex with AtFLS2, we performed coimmunoprecipitation experiments before and after flg22 treatment of *A. thaliana* La-er cell cultures. An antibody raised against AtFLS2 (αAtFLS2) efficiently immunoprecipitated AtFLS2 from solubilized microsomal membranes of Col-0 WT seedlings and La-er cultured cells but not from Δ*fls2* seedlings lacking AtFLS2 (Fig. 1 *A* and *B*), confirming the specificity of the antibody. Furthermore, AtFLS2 was not immunoprecipitated by an unrelated antibody or in the absence of antibody [supporting information (SI) Fig. 5]. αAtFLS2-immunoprecipitated AtFLS2 [confirmed by liquid chromatography-tandem mass spectrometry (LC-MS/MS) analysis; SI Table 1] in equal amounts from microsomes of unelicited and flg22-elicited La-er cultured cells (Fig. 1*B*). Interestingly, a protein of ≈70 kDa coimmunoprecipitated with

Author contributions: A.H. and D.R.H. contributed equally to this work; A.H., D.R.H., and J.P.R. designed research; A.H., D.R.H., S.G.-I., and A.M.E.J. performed research; A.H., D.R.H., S.G.-I., K.H., J.L., J.I.S., S.C.P., and J.P.R. contributed new reagents/analytic tools; A.H., D.R.H., S.G.-I., A.M.E.J., S.C.P., and J.P.R. analyzed data; and A.H., D.R.H., and J.P.R. wrote the paper.

The authors declare no conflict of interest.

Abbreviations: PAMP, pathogen-associated molecular patterns; PTI, PAMP-triggered immunity; RLK, receptor-like kinase; BR, brassinosteroid; SERK, somatic embryogenesis receptor kinase; BAK1, BRT1-associated kinase 1; FLS2, FLAGELLIN-SENSING 2; PRR, pattern-recognition receptor; AOS, active oxygen species; BRI, BR-INSENSITIVE; EV, empty vector; LC-MS/MS, liquid chromatography-tandem mass spectrometry; VIGS, virus-induced gene silencing.

Data deposition: The sequences reported in this paper have been deposited in the GenBank database [accession nos. CK291393 (*NbSerk3*) and CK291392 (*NbSerk2*)].

†To whom correspondence may be addressed. E-mail: heesea@missouri.edu or john.rathjen@tsl.ac.uk.

‖Present address: Department of Biochemistry, University of Missouri, 271H Bond Life Sciences Center, 1201 Rollins Road, Columbia, MO 65211.

This article contains supporting information online at www.pnas.org/cgi/content/full/0705306104/DC1.

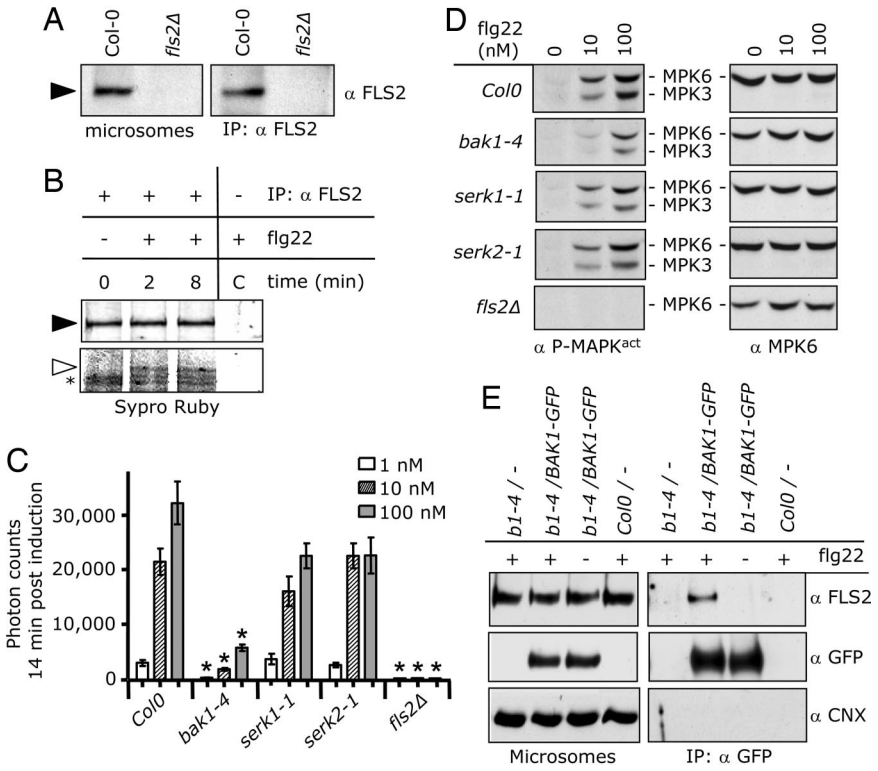


**Fig. 1.** Elicitor-dependent formation of an AtSERK3/BAK1–AtFLS2 complex and requirement for AtSERK3/BAK1 in flg22-dependent responses in *A. thaliana*. (*A*) Specificity of the αAtFLS2 antibody. Solubilized microsomes of Col-0 and Δ*fls2* seedlings were subjected to immunoprecipitation and immunoblot analysis by using αAtFLS2 (αFLS2) antibodies. (*B*) Coimmunoprecipitation of a 70-kDa protein (open arrowhead) with AtFLS2 (closed arrowhead) by using αAtFLS2 antibody after 100 nM flg22 elicitation from La-er cultured cells for the indicated time (in minutes). After separation on SDS/PAGE, immunoprecipitates were stained with Sypro ruby for total proteins. Proteins coimmunoprecipitated independent of flg22-elicitation are indicated by asterisks. (*C*) Dose-dependent AOS production at 14 min after elicitation with increasing flg22 concentrations in WT Col-0, *serk1-1*, *serk2-1*, *bak1-4*, and *fls2*Δ mutant lines, as indicated. Every experiment ($n = 5$) was repeated at least three times with similar results. For this experiment, $n = 5$ samples were analyzed, with an SEM (±) as indicated (error bars). Two sample *t* tests were performed for every experiment comparing each mutant to Col-0 at the same flg22 concentrations. At each flg22 concentration, the *P* values were highly significant ($P < 0.01$) for *bak1-4* and Δ*fls2* mutant but not for *serk1-1* and *serk2-1* ($P \geq 0.097$). Statistical significance is indicated by asterisks. (*D*) Dose-dependent MAPK activation after increasing flg22 concentrations at 15 min in Col-0 (WT), *serk1-1*, *serk2-1*, *bak1-4*, and Δ*fls2* seedlings as shown by immunoblot analysis by using an αp44/42-ERK antibody (αP-MAPK$^{act}$). Individual MAPKs are identified by mass. The same blots were stripped and probed with αMPK6 for equal loading. (*E*) flg22-dependent coimmunoprecipitation of AtFLS2 with AtSERK3/BAK1-GFP after 100 nM flg22 elicitation in *bak1-4* seedlings expressing AtBAK1-GFP (b1-4/BAK1-GFP) but not in nonelicited bak1-4/AtBAK1-GFP or in elicited nontransformed *bak1-4* or Col-0 seedlings. Solubilized membrane proteins were subjected to immunoprecipitation with αGFP antibodies followed by immunoblot analysis with antibodies indicated to the right to detect AtFLS2 (αFLS2), AtBAK1/SERK3-GFP (αGFP), and AtCalnexin (CNX), a membrane ER protein (αCNX).

FLS2 within 2 min of flg22 treatment but not before elicitation (Fig. 1*B*). Sequencing of this 70-kDa protein by LC-MS/MS (SI Table 1) identified four peptides matching members of the SERK family (SI Fig. 6) with roles in plant development (20, 21). Peptide sequence information excluded SERK4 and SERK5 but could not distinguish between SERK1, SERK2 and SERK3/BAK1 (SI Table 2). SERK3/BAK1 functions in hormone signaling via interaction with the BR receptor BRI1 (20, 22–24), whereas SERK1 and SERK2 have redundant functions in anther development (25, 26). Recently, SERK1 has also been implicated in BR signaling (27).

To test whether *SERK1*, *SERK2*, or *SERK3*/*BAK1* were required for AtFLS2-mediated effects, we examined early flg22-dependent responses in *AtSERK1*, *AtSERK2*, and *AtSERK3*/*BAK1* knockout lines. AOS production (Fig. 1*C*) was strongly induced in Col-0, *serk1-1*, and *serk2-1* leaves in a flg22 dose-dependent manner. No statistically significant difference was observed for *serk1-1* or *serk2-1* compared with Col-0 at any of the flg22 concentrations tested, indicating that *SERK1* and *SERK2* did not contribute significantly to the flg22 response. Furthermore, the double mutant *serk1-1serk2-1* was not significantly impaired in flg22-induced AOS production (data not shown). Conversely, the AOS burst was strongly reduced in the *bak1-4* line. Flg22-dependent AOS production was also significantly impaired in a second line containing a mutation in *BAK1* (*bak1-101*; SI Fig. 5), providing independent evidence that lesions in *BAK1* impaired flg22-dependent responses. In contrast to the *fls2*Δ mutant, which was unresponsive to any concentration of flg22, the *bak1* mutants displayed a slight dose-dependent increase in AOS at higher flg22 concentrations but always significantly below that seen in *serk1-1*, *serk2-1*, and Col-0. The minor responses in *bak1* mutants may indicate that FLS2 alone is capable of residual signaling levels, or that another protein(s), possibly a SERK, may partially complement the requirement for AtSERK3/BAK1. Furthermore, the MAPKs AtMPK3 and AtMPK6 were activated in *serk1-1* and *serk2-1* seedlings to similar levels as in Col-0 (Fig. 1*D*). Conversely, MAPK activation was reduced in *bak1-4*. Stripping and reprobing of blots with αMPK6 confirmed the presence of equal amounts of MPK6 in all samples. Similarly, reduced flg22 responses in *bak1-4* were not due to reduced levels of AtFLS2 protein, because equal amounts of AtFLS2 were detected in *bak1-4* and Col-0 microsomes (Fig. 1*E*).

The genetic data implicated *SERK3*/*BAK1* as a component in flg22 signaling, possibly as the 70-kDa protein identified by mass spectrometry in the AtFLS2 complex. Therefore, we used *bak1-4* seedlings transformed with *AtSERK3*/*BAK1* fused to *green fluorescence protein* (*bak1-4*/*BAK1-GFP*) to confirm a potential *in vivo* interaction between AtSERK3/BAK1 and AtFLS2 by additional

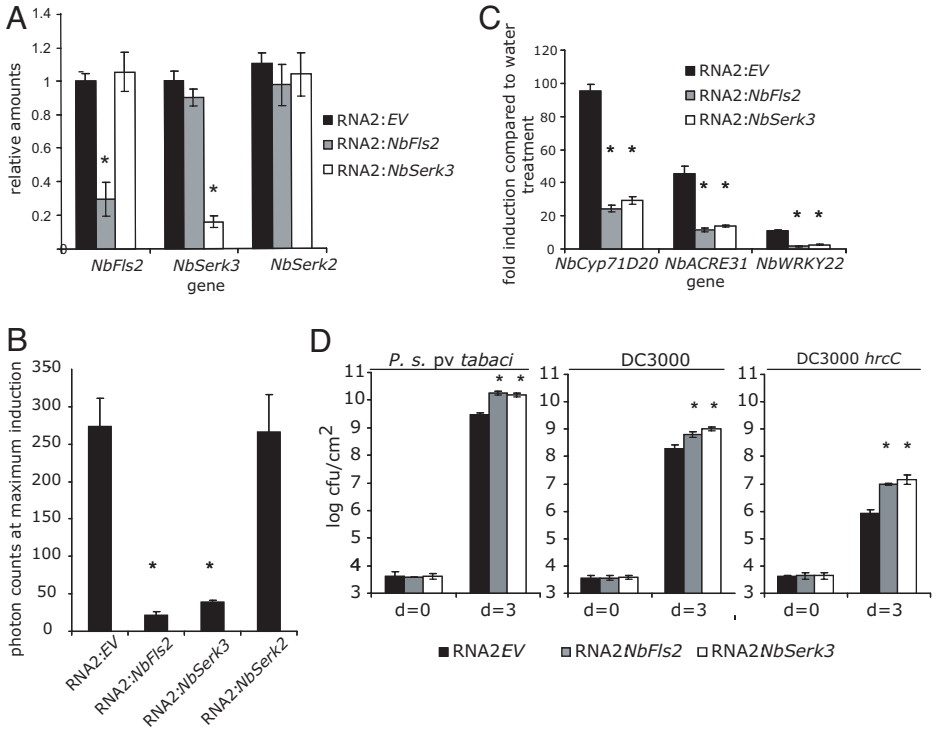


**Fig. 2.** Flagellin-triggered immunity in *N. benthamiana*. (*A*) Quantitative RT-PCR of *NbFls2*, *NbSerk2*, and *NbSerk3* expression in *N. benthamiana* tissue silenced for RNA2:*EV*, RNA2:*NbFls2*, or RNA2:*NbSerk3*. The samples were normalized against the housekeeping gene *NbEF1*$\alpha$. $n = 3$ samples were analyzed per experiment with the SEM (±), as indicated (error bars). For every experiment, two sample *t* tests were performed and showed a significant reduction of the respective gene with $P \leq 0.01$. (*B*) AOS burst in *N. benthamiana* tissue silenced for *EV*, *NbFls2*, *NbSerk3*, and *NbSerk2* induced by 50 nM flg22. For this experiment, $n = 12$ samples were analyzed, with an SEM (±) as indicated (error bars). Two sample *t* tests show that *EV* is significantly different from *NbFls2* and *NbSerk3* by $P \leq 0.05$. (*C*) Quantitative RT-PCR analysis of defense gene expression induced by 100 nM flg22 for 30 min in tissue silenced for *EV*, *NbFls2*, or *NbSerk3* relative to untreated tissue. All samples were normalized against the housekeeping gene *NbEF1*$\alpha$. $n = 3$ samples were analyzed per experiment with the SEM (±), as indicated (error bars). For every experiment, two sample *t* tests were performed and showed that *EV* is significantly different from *NbFls2* and *NbSerk3* by $P \leq 0.01$. (*D*) Bacterial growth curves with three *P. syringae* strains on *N. benthamiana* silenced for *EV*, *NbFls2*, or *NbSerk3* at 0 and 3 days post infiltration. $n = 3$ samples were analyzed per experiment with the SEM (±), as indicated (error bars). For every experiment, two sample *t* tests were performed and showed that *EV* is significantly different from *NbFls2* and *NbSerk3* by $P \leq 0.05$. Every experiment of Fig. 2 was repeated at least three times with similar results. Statistical significance is indicated by asterisks.

coimmunoprecipitation analysis. Using $\alpha$GFP antibodies, AtFLS2 coimmunoprecipitated with BAK1-GFP only after flg22 elicitation but not after a water control treatment (Fig. 1*E*), confirming the stimulus-specific interaction of the two proteins. A number of controls demonstrated the specificity of this result. Equal amounts of AtBAK1-GFP were immunoprecipitated from flg22-elicited and nonelicited *bak1-4/BAK1-GFP* seedlings but not from *bak1-4* or Col-0 seedlings. Similar levels of AtFLS2 were present in all seedlings, and $\alpha$GFP antibodies did not immunoprecipitate AtFLS2 from *bak1-4* or Col-0 after flg22 treatment. Finally, the ER membrane protein AtCalnexin (28) did not coimmunoprecipitate with AtBAK1-GFP. These results indicated that the RLKs AtFLS2 and AtSERK3/BAK1 form an elicitor-dependent complex. Although we cannot exclude that AtSERK1 and/or AtSERK2 may also interact with AtFLS2, the genetic data demonstrate that AtSERK3/BAK1 is the main SERK contributing to flg22-dependent responses in *A. thaliana*.

***NbSerk3/BAK1* Is Required for Flagellin-Triggered Immunity in *N. benthamiana*.** Flagellin perception and responses have been observed in a variety of plant species (13, 15, 16). In *A. thaliana*, flagellin recognition contributes only weakly to PTI against bacterial growth (17). In contrast, the growth of several bacterial strains on the Solanaceous species *N. benthamiana* is strongly restricted by *NbFls2* (16), making it an excellent system to determine whether SERK3/BAK1 functions in PTI against bacteria. First, we established that, as in *Arabidopsis* (Fig. 1 *C* and *D*), *SERK3/BAK1* is required for *NbFls2*-dependent responses in *N. benthamiana*. To this end, we generated a construct for virus-induced gene silencing (VIGS) of *NbSerk3* based on a gene fragment cloned from *N. benthamiana* (SI Fig. 6). This construct silenced *NbSerk3* but had no effect on the mRNA levels of *NbFls2* and a putative *NbSerk2* ortholog (Fig. 2*A*). Interestingly, *NbSerk3*-silenced plants were slightly stunted with weakly distorted leaves (SI Fig. 6). These phenotypes are reminiscent of *SERK3/BAK1* knockouts in *A. thaliana* attributable to defects in BR perception (22, 23). Gene expression studies confirmed that these silenced plants were unresponsive to treatment with exogenous brassinolide (data not shown). Consistent with the reduced responses to flg22 observed in *A. thaliana* Δ*bak1* plants, silencing of *NbSerk3* severely reduced flg22-dependent AOS production (Fig. 2*B*) and activation of the MAPK salicylic acid-induced protein kinase, the *Nicotiana* ortholog of AtMAPK6 (SI Fig. 6), as compared with plants silenced with the empty vector (*EV*) construct. The specificity of gene silencing was confirmed by using a second VIGS construct targeting a distinct region of *NbSerk3* (data not shown). Moreover, consistent with the *Arabidopsis* data, silencing of the *NbSerk2* ortholog did not affect flg22-elicited AOS production (Fig. 2*B*). An important plant response to PAMPs and pathogens is a changed pattern of gene expression. We found that the marker genes *NbWRKY22*, *NbCyp71D20*, and *NbACRE31* (18) were up-regulated within 30 min of flg22 treatment in WT and *EV*-silenced *N. benthamiana* (Fig. 2*C* and SI Fig. 6). In contrast,

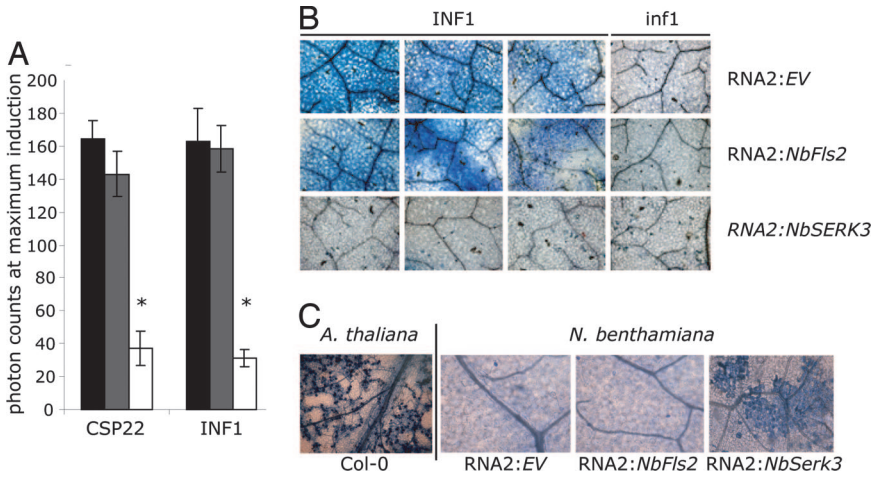


**Fig. 3.** *NbSerk3* is required for multiple PAMP-mediated responses in *N. benthamiana*. (*A*) AOS burst in *N. benthamiana* tissue silenced for *EV* (black), *NbFls2* (gray), or *NbSerk3* (white) treated with 100 nM CSP22 or 10 $\mu$g/ml INF1. For each treatment, $n = 12$ samples were analyzed, with an SEM ($\pm$) as indicated (error bars). Two sample *t* tests show that *EV* and *NbFls2* are significantly different from *NbSerk3* by $P \leq 0.05$ in each treatment. Statistical significance is indicated by asterisks. (*B*) Trypan blue staining indicative of cell death of *EV*, *NbFls2*, or *NbSerk3* silenced *N. benthamiana* treated with 100 $\mu$g/ml INF1 or inf1. (*C*) Trypan blue staining was used to visualize cell death and oomycete structures on *EV*, *NbFls2*, or *NbSerk3* silenced *N. benthamiana* tissue infected with *H. parasitica*. *A. thaliana* Col-0 tissue infected with *H. parasitica* was used as an infection control. The pictures were taken 3 weeks after inoculation. The experiment was performed three times with similar results.

silencing of *NbFls2* or *NbSerk3* severely reduced up-regulation of these genes. Overall, the data confirm a role for SERK3/BAK1 in flg22-mediated responses in two distantly related species.

***NbSerk3/BAK1* Is Required for Multiple PAMP-Mediated Responses in *N. benthamiana*.** To investigate a possible role of *NbSerk3* in bacterial PTI, we analyzed whether *NbSerk3* silencing also affected growth of different *Pseudomonas syringae* strains on *N. benthamiana*. We selected the unadapted pathogen *P. syringae* pv. *tomato* DC3000 (*Pto* DC3000) and the nonpathogenic *hrcC* derivative of *Pto* DC3000. Silencing of *NbFls2* enhanced the growth of each strain relative to growth on *EV*-silenced plants. Importantly, silencing of *NbSerk3* provided a growth advantage similar to that caused by *NbFls2* silencing (Fig. 2*D*). These data reinforce the importance of flagellin as a restrictive PAMP on *N. benthamiana* and *NbSerk3* as a key component of the *NbFls2* pathway. The growth of the adapted pathogen *P. syringae* pv. *tabaci* 11528 (*Pta* 11528) was similarly enhanced on plants silenced for *NbFls2* or *NbSerk3*. That the greatest increase in bacterial growth was observed with the nonpathogenic *Pto* DC3000 *hrcC* is consistent with a lack of PTI suppression because of its inability to secrete virulence effectors into the host cell (29). These results demonstrate that *NbSerk3* is a new component of PTI.

To determine whether a role for *NbSerk3* in PAMP signaling extends beyond flg22 responses, we examined the AOS burst induced by other PAMPs, including the CSP22 peptide derived from bacterial cold-shock protein (7) and the oomycete elicitor INF1 (30). Either elicitor induced AOS in *N. benthamiana* plants silenced for *EV* or *NbFls2* (Fig. 3*A*). Strikingly, both elicitors showed reduced AOS production on *NbSerk3*-silenced plants. In addition, INF1 characteristically induces a cell death response on *Nicotiana* spp. known as the hypersensitive response (HR) (31). As expected, INF1 infiltration caused HR on *N. benthamiana* plants silenced for *EV* or *NbFls2* within 24 h as shown by trypan blue staining indicative of cell death (Fig. 3*B*). This HR was specific to INF1, because the inactive inf1 mutant protein did not induce cell death (30). INF1 did not cause HR in *NbSerk3*-silenced plants. However, the silenced plants were capable of an HR, because coexpression of the bacterial effector *avrPto* in plants containing the resistance gene *Pto* lead to a characteristic HR (32), regardless of whether the plants were silenced for *EV*, *NbFls2*, or *NbSerk3* (SI Fig. 6). Overall, the data suggest participation of *NbSerk3*/*Bak1* in multiple PRR pathways.

The strong requirement for *NbSerk3* for perception of multiple PAMPs indicated a general role for this gene in immunity. To test this hypothesis, we chose the oomycete *Hyaloperonospora parasitica* (*Hp*) Waco9, an obligate biotroph that is pathogenic on *A. thaliana* Col-0 but is unable to infect *N. benthamiana*. As a positive control, we sprayed Col-0 leaves with an *Hp* Waco9 spore suspension and allowed oomycete development. Three weeks after inoculation, trypan blue staining of the inoculated leaves revealed successful infection, resulting in spore formation (Fig. 3*C*). Similar inoculation of *N. benthamiana* leaves silenced for *EV* or *NbFls2* did not result in infection. Conversely, inoculation of *NbSerk3*-silenced plants caused cell death indicative of successful penetration on 9/10 leaves, compared with 0/10 leaves for the negative controls. However, *Hp* Waco9 sporulation was not observed in *NbSerk3*-silenced plants, demonstrating that the pathogen life cycle was not completed.

## Conclusions

Our data identify SERK3/BAK1 as a factor involved in PTI. SERK3/BAK1 is required for early PAMP responses and rapidly enters a flg22-induced complex. We therefore speculate that in PAMP responses, SERK3/BAK1 acts similarly to its role in BR signaling as a partner of the BRI1 receptor (33). In our model (SI Fig. 4), SERK3/BAK1 may function in a complex with FLS2 and possibly other PRRs to provide a link between PAMP perception and subsequent early defense responses. Whether either RLK transactivates the other and/or recruits downstream factors to the complex remains unknown. Previous studies have shown a major role for FLS2 in flg22 binding (13, 14), but it is formally possible that SERK3/BAK1 also contributes to ligand binding. Interestingly, FLS2 belongs to the non-RD kinases with proposed roles in innate immunity, whereas SERK3/BAK1 is an RD kinase, although the significance of this observation remains to be determined (1). The involvement of SERK3/BAK1 in PTI provides further evidence of commonalities between plant immunity and BR signaling, consistent with the known role of tomato SR160/tBRI1 in systemic wound signaling (34). BR signaling plays roles in cell expansion and division, differentiation, and reproductive development (35). In contrast, PAMP signaling is important for resistance to pathogens through activation of several defense-associated responses. So far, shared pathway components or responses between BR signaling

and PAMP signaling have not been reported. Comparisons of gene expression in the presence of either brassinolide or flg22 revealed no apparent overlap in expression patterns (18, 36). However, it is interesting to note that application of flg22 to the medium leads to a growth inhibition phenotype in *Arabidopsis* seedlings (37). This phenotype could suggest interplay between BR and flagellin signaling, potentially mediated by BAK1. Finally, the identification of a conserved component of multiple PAMP-PRR response pathways makes this protein a likely target of pathogen virulence factors to suppress PTI.

## Materials and Methods

**Plant Materials and Growth Conditions.** *A. thaliana* seeds were grown on 0.5× Murashige–Skoog plates containing 1% sucrose for 7–8 days at 22°C under continuous light in environment-controlled chambers. For elicitation assays, seedlings were transferred into water overnight. *A. thaliana* plants were grown at 22°C in a 10-h light/14-h dark cycle in controlled environment chambers. All mutant alleles were in the Col-0 background. *serk1-1* and *serk2-1* have been described (26). *bak1-4* (SALK_116202; T-DNA insertion in the ninth exon), *bak1-101* (SALK_034523), and Δ*fls2* (SALK_093905; T-DNA insertion in the first exon) were obtained from the Signal collection [Salk Institute, La Jolla, CA (38)] and confirmed by RT-PCR and immunoblot analyses, respectively. La-er cultured cells were maintained as described (10). *Agrobacterium*-mediated transformation of Col-0 with pBIB-BASTA-35S-BAK1-GFP was done as described (22). To obtain pBIB-BASTA-35S-BAK1-GFP, a KpnI and SacI fragment containing BAK1-GFP was isolated from pKAN-35S-BAK1-GFP (22) and ligated into KpnI and SacI sites of pBIB-BASTA-35S.

**Bacterial Strains.** *A. tumefaciens* GV3101 was used for VIGS, transformed with the respective silencing construct. *Escherichia coli* strain DH5α transformed with pFB53 was used for expression of INF1 and inf1. *P. syringae* strains used are indicated in the text.

**Purification of INF1.** INF1 was prepared from *E. coli* expressing the *Pseudomonas infestans Inf1* gene as described (30) and used to elicit an HR (100 μg/ml INF1) on *N. benthamiana* plants. Control preparations from *E. coli* expressing a mutated *inf1* gene did not induce an HR in these experiments.

**Measurement of AOS Generation.** In *N. benthamiana*, leaf discs (0.38 $cm^2$; one per well) were floated on water overnight. AOS released by the leaf tissue were measured by a luminol-dependent assay (39). The water was replaced with 500 μl of a solution containing 20 μM luminol (Sigma, St. Louis, MO) and 1 μg of horseradish peroxidase (Fluka, Buchs, Switzerland). AOS were elicited with flg22, INF1, or CSP22. Luminescence was measured by using a Photek (East Sussex, U.K.) camera system over time, and data were selected at maximum intensity of the response. In *A. thaliana*, leaf discs (0.6 $cm^2$) of 3- to 4-week-old plants were cut into nine small pieces. Using a Veritas microplate luminometer (Turner Biosystem, Sunnyvale, CA), AOS production was measured after elicitation with 1, 10, or 100 nM flg22 in a luminol based assay as described (40).

**Antibodies and Immunoblot Analysis.** Peptides used for antibody production and affinity purifications were as follows: CKANSFREDRNEDREV of AtFLS2, CSRRLSDEVQNKPPE of an unrelated protein (AtCPK1), and both peptides MDGGSGQPAADTEMT and LAFNPEYQQ of AtMKP6. Polyclonal antibodies against synthetic peptides were produced in rabbits (Eurogentec, Seraing, Belgium). With the exception of the αMPK6 antibody (used as crude serum), peptide antibodies were affinity-purified against the individual peptide by Eurogentec according to the company's specifications.

Immunoblot analysis was basically performed as described (40) except that (*i*) proteins were separated on 7.5% or 8% SDS/PAGE, (*ii*) membranes probed with α-p44/42-ERK were incubated with TBS instead of PBS buffers, and (*iii*) signals were visualized by using ECL systems (ECL or SuperSignal West Femto). The following antibody concentrations were used: αAtFLS2, 1:3,000; αMPK6, 1:3,000; αrabbitGFP, 1:2,000 (Medical and Biological Laboratories, Woburn, MA; JM-3999–100); αcalnexin, 1:2,000 (28); αphospho-p44/42-ERK, 1:3,000 (αPMAPKact; Cell Signaling Technology, Danvers, MA).

**Immunoprecipitation and SDS/PAGE Staining.** Protein isolation and immunoprecipitation steps were done on ice or at 4°C. Approximately 120 seedlings or 50 ml of La-er cultured cells were homogenized on ice in Buffer H (50 mM Hepes, pH 7.5/250 mM sucrose/15 mM EDTA/5% glycerol/0.5% polyvinylpyrrolidone K25/1 mM phenylmethylsulfonyl fluoride/2 μg/ml leupeptin/50 mM sodium pyrophosphate/25 mM sodium fluoride/1 mM sodium molybdate/10 nM calyculin) containing 3 mM DTT. Isolated microsomes (19) were resuspended in buffer H and solubilized in 0.5% or 1% Nonidet P-40 (Roche, Indianapolis, IN) for 30 min on ice at a concentration of 1.5 mg of protein per milliliter, separated into a soluble (S3) and insoluble faction (P3) by centrifugation (30 min, 100,000 ×*g*), precleared with protein A-Sepharose beads (Sigma), and incubated with 4–5 μg of αFLS2 affinity purified in the presence of protein A-Sepharose beads for 1 h at 4°C. For immunoprecipitation of BAK1-GFP, solubilized microsomes were incubated overnight with 20 μl of agarose-conjugated αGFP (rat monoclonal antibody; Medical and Biological Laboratories, D153-8). After three washing steps with buffer H containing 0.2% Nonidet P-40, immunoprecipitates were analyzed by immunoblot analyses.

Large-scale immunoprecipitations were performed as described above except that, per timepoint (elicitation with 0.1 μM flg22 for 0, 2, and 8 min), 130 mg of microsomal protein was isolated from 750 ml of La-er cultured cells, solubilized at 2.7 mg of protein per milliliter in buffer H containing 0.5% Nonidet P-40, and incubated overnight with 50 μg of αAtFLS2. Immunoprecipitates were separated on 10% SDS/PAGE, visualized with Sypro Ruby stain (Invitrogen, Carlsbad, CA) according to the manufacturer's specifications, and subsequently incubated with colloidal Coomassie blue G-250 (SERVA Blue G, Sigma) for LC-MS/MS analysis. Protein bands of interest were cut out as tightly as possible with a razor blade for LC-MS/MS analysis.

**LC-MS/MS Analysis.** Proteins were digested in gel slices (trypsin; Promega, Southampton, U.K.) after reduction with DTT and alkylation with iodoacetamide (Sigma). Nanoflow LC-MS/MS analysis was performed by using an LTQ mass spectrometer (Thermo Fisher, Hemel Hempstead, U.K.) with automated data-dependent acquisition. A nanoflow-HPLC system (Surveyor, Thermo Electron) was used to deliver a flow rate of ≈250 nl $min^{-1}$ to the mass spectrometer. Peptides were desalted by using a precolumn (C18 pepmap100; Dionex Corp., Sunnyvale, CA), which was switched in line to the analytical self-packed C18, 8-cm analytical column (Picotip 75-μm i.d., 15-μm tip; New Objective, Woburn, MA). Peptides were eluted by a gradient of 2–30% acetonitrile over 40 min. The mass spectrometer was operated in positive ion mode with a nanospray source and a capillary temperature of 200°C; no sheath gas was used, and the source voltage and focusing voltages were optimized for the transmission of angiotensin. Data-dependent analysis consisted of six most-abundant ions in each cycle: MS mass-to-charge ratio (*m*/*z*) 300–2,000, minimum signal 1,000, collision energy 25, five repeat hits, and 300-sec exclusion. Isolation width for MS2 analysis was 2 *m*/*z*. MS3 were triggered by neutral loss of 32 or 49 from the parent ion.

**MAPK Activation.** After elicitation with 0.01, 0.1, and 1 μM flg22 for 15 min, seedlings were ground in buffer H containing 3 mM

DTT. Total proteins were subjected to immunoblot analysis by using the αP-MAPK$^{act}$. Blots were stripped with 0.1 M glycine, pH 2.5, and reprobed with αMPK6 antibodies.

**In-Gel Kinase Assay.** In-gel kinase assays were performed as described (41).

**RNA Extractions.** Total RNA was extracted by using TRIzol-Reagent (Sigma), and the absence of genomic DNA was checked by PCR amplification of the housekeeping NbEF1α gene by using 2.5 μg of RNA.

**Quantitative RT-PCRs.** Leaf discs were soaked overnight in water, then treated with 100 nM flg22. For analysis of gene expression, first-strand cDNA was synthesized from 2.5 μg of RNA by using SuperScript RNA H$^-$ Reverse Transcriptase (Invitrogen) and oligo(dT) primer, according to the manufacturer's instructions. One microliter of the RT reaction was used for each PCR. Primers for genes used here are shown as follows: *NbSerk3*, 5′-TCCTGACGGACCATCTCCTCTTT-3′ and 5′-GCTCATAACTGGGCAAAGGGCTT-3′; *NbSerk2*, 5′-AATCTAGGTTTTAGGTGGTGGCGG-3′ and 5′-CTGAAGCTTGCCCAATGTGTCAG-3′; *NbFls2*, 5′-CTGTGTACAAGGGTAGACTGGAAGATGG-3′ and 5′-GGAGAGGTGCAAGGACAAAGCCAATTT-3′; *NbAcre31*, 5′-AAGGTCCCGTCTTCGTCGGATCTTCG-3′ and 5′-AAGAATTCGGCCATCGTGATCTTGGTC-3′; *NbCyp71D20*, 5′-AAGGTCCACCGCACCATGTCCTTAGAG-3′ and 5′-AAGAATTCCTTGCCCCTTGAGTACTTGC-3′; *NbWrky22*, 5′-AAGGTCCGGGATCTACATGCGGTGGT-3′ and 5′-AAGAATTCCGGGTCGGATCTATTTCG-3′; and *NbEF1α*, 5′-AAGGTCCAGTATGCCTGGGTGCTTGAC-3′ and 5′-AAGAATTCACAGGGAC AGTTCCAATACCA-3′.

PCR parameters were as follows: 3 min, 94°C (first cycle); 30 sec, 94°C; 30 s, 52°C; 1 min, 72°C (28–40 cycles); and 15 min, 72°C (last cycle). All PCR products were loaded in 1% agarose gels and visualized after ethidium bromide staining. For quantitative PCR, cDNAs were combined with SYBR master mix. PCRs were performed in triplicate with a PTC-200 Peltier Thermal Cycler (MJ Research, Waltham, MA), and the data were collected and analyzed with Chromo 4 Continuous Fluorescence detection system. The *NbEF1α* RNA was analyzed as an internal control and used to normalize the values for transcript abundance.

**Trypan Blue Staining for Cell Death and Oomycetes Structures.** Leaves were submerged in trypan blue staining solution (6 vol of ethanol, 1 vol of water, 1 vol of lactic acid, 1 vol of glycerol, 1 vol of phenol, 0.067% wt/vol trypan blue) in universal tubes and heated in a boiling water bath for 2 min. After cooling, the solution was replaced with chloral hydrate (2.5 g/ml), and samples were shaken until leaves were fully destained. For microscopy, the chloral hydrate was replaced with 60% glycerol.

**Bacterial Growth Curves.** For bacterial growth curves, *P. syringae* strains were grown overnight at 28°C with shaking in L medium (10 g/liter bactotryptone/5 g/liter yeast extract/5 g/liter NaCl/1 g/liter NaCl) containing the appropriate antibiotics. Bacterial suspensions in 10 mM $MgCl_2$ and 0.01% Silwet were infiltrated at $2 \times 10^4$ cfu/ml by vacuum infiltration. Leaf discs were harvested at 1 and 3 days after inoculation and ground in 10 mM $MgCl_2$. The cfu/cm$^2$ were determined by plating serial dilutions of leaf extracts on L agar plates containing the appropriate antibiotics. Each data point represents average bacterial numbers of three replicates, and error bars indicate SEMs.

***H. parasitica* Waco9 Infections.** *N. benthamiana* plants were spray-inoculated densely at a concentration of $4 \times 10^4$ spores per millilter 1 week after silencing. Subsequently, the plants were covered by a plastic lid to maintain humidity and transferred to growth cabinets for 3 weeks at a constant temperature of 16°C.

**VIGS.** VIGS was performed by using a tobacco rattle virus vector as described (42). For *NbSerk3* silencing, the following primers were used: 5′-gaattcGTGAGG-GTGGTGAGCGGGATAAT-3′ and 5′-ctcgagGCTCATAACTGGGCAAAGGG-CTT-3′; and for the alternative fragment, 5′-gaattcTTGTGCTTCTACAG-CCATTCCTGC-3′ and 5′-ctcgagGGGTCAAAGGACTTCTGAAGGACA-3′. For *NbSerk2* silencing, we used 5′-gaattcTGACTGTTGAAGACGTGGCAT-GTG-3′ and 5′-ctcgagCTGAAGCTTGCCCAATGTGTCAG-3′.

We thank Dr. L. Serazetdinova for identifying the *fls2Δ* T-DNA line; Dr. T. Nühse (Sainsbury Laboratory) for providing elicited La-er microsomes for large-scale immunoprecipitation experiments and discussions; Dr. N. Hoffman (Sainsbury Laboratory) for the calnexin antibody; Dr. M. Montero for help with VIGS; K. Walker, M. Benitez, and A. Rougon for technical help; Prof. G. Weisman and his laboratory for support and discussion; Dr. P. Moffett and Prof. J. Walker for discussions; and the Salk Institute, the *Arabidopsis* Biological Resource Center (Ohio State University, Columbus, OH) and the European *Arabidopsis* Stock Centre (NASC, University of Nottingham, Nottingham, U.K.) for providing the T-DNA insertion lines. This work was supported by the Gatsby Charitable Foundation (J.P.R. and S.C.P.) and by start-up funds from the Food for 21 Century, University of Missouri (A.H.).

1. Dardick C, Ronald P (2006) *PLoS Pathog* 2:e2.
2. Shiu SH, Karlowski WM, Pan R, Tzeng YH, Mayer KF, Li WH (2004) *Plant Cell* 16:1220–1234.
3. Gomez-Gomez L, Boller T (2000) *Mol Cell* 5:1003–1011.
4. Zipfel C, Kunze G, Chinchilla D, Caniard A, Jones JD, Boller T, Felix G (2006) *Cell* 125:749–760.
5. Peck SC, Nuhse TS, Hess D, Iglesias A, Meins F, Boller T (2001) *Plant Cell* 13:1467–1475.
6. Sasabe M, Takeuchi K, Kamoun S, Ichinose Y, Govers F, Toyoda K, Shiraishi T, Yamada T (2000) *Eur J Biochem* 267:5005–5013.
7. Felix G, Boller T (2003) *J Biol Chem* 278:6201–6208.
8. Gomez-Gomez L, Bauer Z, Boller T (2001) *Plant Cell* 13:1155–1163.
9. Chisholm ST, Coaker G, Day B, Staskawicz BJ (2006) *Cell* 124:803–814.
10. Nuhse TS, Peck SC, Hirt H, Boller T (2000) *J Biol Chem* 275:7521–7526.
11. Asai T, Tena G, Plotnikova J, Willmann MR, Chiu WL, Gomez-Gomez L, Boller T, Ausubel FM, Sheen J (2002) *Nature* 415:977–983.
12. Gomez-Gomez L, Boller T (2002) *Trends Plants Sci* 7:251–256.
13. Chinchilla D, Bauer Z, Regenass M, Boller T, Felix G (2006) *Plant Cell* 18:465–476.
14. Bauer Z, Gomez-Gomez L, Boller T, Felix G (2001) *J Biol Chem* 276:45669–45676.
15. Felix G, Duran JD, Volko S, Boller T (1999) *Plant J* 18:265–276.
16. Hann DR, Rathjen JP (2007) *Plant J* 49:607–618.
17. Zipfel C, Robatzek S, Navarro L, Oakeley EJ, Jones JD, Felix G, Boller T (2004) *Nature* 428:764–767.
18. Navarro L, Zipfel C, Rowland O, Keller I, Robatzek S, Boller T, Jones JD (2004) *Plant Physiol* 135:1113–1128.
19. Nuhse TS, Boller T, Peck SC (2003) *J Biol Chem* 278:45248–45254.
20. Russinova E, Borst JW, Kwaaitaal M, Cano-Delgado A, Yin Y, Chory J, de Vries SC (2004) *Plant Cell* 16:3216–3229.
21. Shiu S-H, Bleecker AB (2001) *Proc Natl Acad Sci USA* 98:10763–10768.
22. Li J, Wen J, Lease KA, Doke JT, Tax FE, Walker JC (2002) *Cell* 110:213–222.
23. Nam KH, Li J (2002) *Cell* 110:203–212.
24. Wang X, Goshe MB, Soderblom EJ, Phinney BS, Kuchar JA, Li J, Asami T, Yoshida S, Huber SC, Clouse SD (2005) *Plant Cell* 17:1685–1703.
25. Albrecht C, Russinova E, Hecht V, Baaijens E, de Vries S (2005) *Plant Cell* 17:3337–3349.
26. Colcombet J, Boisson-Dernier A, Ros-Palau R, Vera CE, Schroeder JI (2005) *Plant Cell* 17:3350–3361.
27. Karlova R, Boeren S, Russinova E, Aker J, Vervoort J, de Vries S (2006) *Plant Cell* 18:626–638.
28. Huang L, Franklin AE, Hoffman NE (1993) *J Biol Chem* 268:6560–6566.
29. Roine E, Wei W, Yuan J, Nurmiaho-Lassila EL, Kalkkinen N, Romantschuk M, He SY (1997) *Proc Natl Acad Sci USA* 94:3459–3464.
30. Kamoun S, van West P, de Jong AJ, de Groot KE, Vleeshouwers VG, Govers F (1997) *Mol Plant–Microbe Interact* 10:13–20.
31. Kamoun S, van West P, Vleeshouwers VG, de Groot KE, Govers F (1998) *Plant Cell* 10:1413–1426.
32. Pedley KF, Martin GB (2003) *Annu Rev Phytopathol* 41:215–243.
33. Kinoshita T, Cano-Delgado A, Seto H, Hiranuma S, Fujioka S, Yoshida S, Chory J (2005) *Nature* 433:167–171.
34. Scheer JM, Ryan CA, Jr. (2002) *Proc Natl Acad Sci USA* 99:9585–9590.
35. Belkhadir Y, Chory J (2006) *Science* 314:1410–1411.
36. Lisso J, Steinhauser D, Altmann T, Kopka J, Mussig C (2005) *Nucleic Acids Res* 33:2685–2696.
37. Gomez-Gomez L, Felix G, Boller T (1999) *Plant J* 18:277–284.
38. Alonso JM, Stepanova AN, Leisse TJ, Kim CJ, Chen H, Shinn P, Stevenson DK, Zimmerman J, Barajas P, Cheuk R, *et al.* (2003) *Science* 301:653–657.
39. Keppler LD, Atkinson MM, Baker CJ (1989) *Phytopathology* 79:974–978.
40. Heese A, Ludwig AA, Jones JD (2005) *Plant Physiol* 138:2406–2416.
41. Suzuki K, Shinshi H (1995) *Plant Cell* 7:639–647.
42. Peart JR, Cook G, Feys BJ, Parker JE, Baulcombe DC (2002) *Plant J* 29:569–579.